Received: 7 November 2018 | Revised: 14 March 2019 | Accepted: 19 March 2019

DOI: 10.1002/jmor.20986

RESEARCH ARTICLE

JOURNAL OF morphology WILEY

Powering the hagfish "bite": The functional morphology of the retractor complex of two hagfish feeding apparatuses

Benjamin Luke Clubb[1] | Andrew Jonathan Clark[2] | Theodore Akira Uyeno[1]

[1]Department of Biology, Valdosta State University, Valdosta, Georgia

[2]Department of Biology, College of Charleston, Charleston, South Carolina

Correspondence
Theodore Akira Uyeno, Department of Biology, Valdosta State University, 1500 N. Patterson St., Valdosta, GA 31698.
Email: tauyeno@valdosta.edu

Funding information
National Science Foundation, Division of Integrative Organismal Systems, Grant/Award Number: 1354788; The Graduate School at Valdosta State University, Student Travel Grant; NOAA Fisheries; Howard University

Abstract

Hagfish use forceful retractions of a dental plate to shear and ingest food. Retractile force is generated by the retractor muscle complex of the posterior hagfish feeding apparatus (HFA). While gross morphological descriptions exist, the organization of muscle and connective tissue fibers that form the soft tissue retractor complex do not. In this study, we used paraffin histology to prepare serial sections of Pacific (*Eptatretus stoutii*, Lockington, 1879) and Atlantic (*Myxine glutinosa*, Linnaeus, 1758) hagfishes in order to describe constituent soft tissue anatomy and fiber orientations. We generated 3D reconstructions in which digitized sections were segmented and fitted to volumetric scans of retractor complexes taken prior to microtomy. These models confirmed that the retractor complex is composed of a perpendicularis muscle that fits within the eye of a needle-shaped clavatus muscle, which anteriorly bears the dental plate tendon, and in turn fits within a sleeve-like tubulatus muscle. Analysis of fiber orientations within these muscles resulted in novel functional hypotheses: (a) The tubulatus muscle represents a novel tubular bipennate muscle with a considerable physiological cross-sectional area. Its activation may indirectly create tension in the dental plate tendon: as the tubulatus muscle forcefully extends, it displaces the terminal bulb and the clavatus muscle posteriorly. (b) Within the HFA terminal bulb, the muscle fibers of the clavatus and perpendicularis muscles are mutually perpendicular and may cocontract to form a swelling stopper knot-like muscular complex that resists being pulled through the tubulatus muscle. (c) While overall feeding apparatus muscle morphology is conserved, the physiological cross-sectional area of the tubulatus muscle in *E. stoutii*, is relatively larger than that of *M. glutinosa*, suggesting a more forceful retraction. The tubular bipennate construction of the tubulatus may represent a novel soft robotic actuator design.

KEYWORDS

3-dimensional reconstruction, histology, muscular hydrostat, *Myxine*, *Eptatretus*

1 | INTRODUCTION

The feeding strategies, both predatory and scavenging, of the jawless hagfish requires forceful removal of ingestible chunks of tissue from prey. In jawed organisms, this force is easily generated and applied by a biting system that can be simply modeled as a third-order lever (Figure 1). This type of biting system is successful because having rigid jaws, that are connected by a compression-resistant joint, enables an organism to apply opposing bite and bite reaction forces through a closed kinematic loop (Uyeno & Clark, 2015). However, hagfishes lack rigid opposable jaws and

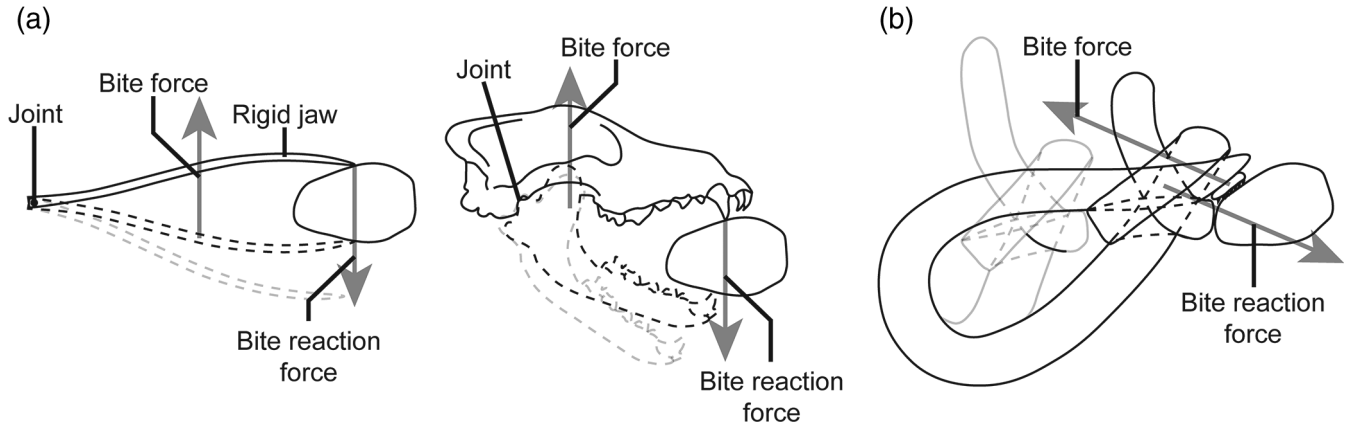

FIGURE 1 Two biting systems modeled as two-dimensional, third-order levers (adapted from Uyeno & Clark, 2015). (a) On the left is a pair of forceps, which in this case, bite force is applied between the joint and the distal end of the jaw. The opposable jaw transfers equal bite reaction forces creating a closed kinematic loop resulting in a grip. On the right is an analogous biting system of a wolf skull, in which muscular force is applied between the temporomandibular joint and the load where food is gripped by teeth. (b) A hagfish creating a closed kinematic loop in which retractile bite forces are opposed by bite reaction forces transferred via body knots

thus seem incapable of closing their biting system's kinematic loop and completing a successful bite (Figure 1). Yet, Clark and Summers (2007) have observed hagfish removing flesh from secured food items with the force approaching that of a gnathostome bite. Uyeno and Clark (2015) suggest hagfishes can accomplish this feat using coordinated movements of a unique feeding apparatus and opposing body knot loops that can be pressed against food to close the kinematic loop.

The hagfish feeding apparatus (HFA) is a highly deformable cylinder composed of muscle and connective tissue (Figure 2). The HFA comprises a cartilaginous dental plate bearing a formidable array of recurved keratinous teeth, a supportive cartilaginous basal plate, and their associated musculature (Figure 2). Current anatomical descriptions (e.g., Clark, Maravilla, & Summers, 2010; Uyeno & Clark, 2015) typically consider the HFA as being divided into functionally and morphologically distinct anterior and posterior halves (Figure 2). Here, we use terminology used by Dawson (1963). The anterior half is comprised of the anterior and middle divisions of the basal plate, the dental plate, and the deep and superficial protractor muscles (Figure 2). Cole (1907) noted and Dawson (1963) confirmed that these deep and superficial protractor muscles are responsible for the protrusion and unfolding of the dental plate halves. Contractions of these muscles generate forces that move the dental plate anteriorly across the basal plate where it exits the mouth and unfolds to contact prey (Figure 3). The posterior half (hereafter referred to as the retractor complex) is composed of three muscles with different fiber orientations, collectively surrounded by a thin connective tissue sheath: the clavatus, the tubulatus, and the perpendicularis muscles (Figure 2). Dawson (1963) noted that these muscles generate the forces used to drive the teeth into prey, tear a chunk of flesh from the prey, and then withdraw the dental plate and extracted tissue back into the mouth for ingestion (Figure 3). However, the roles of each muscle and the interplay between simultaneously contracting muscles in the retractor complex remain poorly understood.

There have been a number of attempts to both describe the HFA and assign functional postulates to various components of the retractor complex. The earliest functional assessment was brought forth by Fürbringer (1875). Fürbringer's "sliding-core" hypothesis (Figure 4) describes a mechanism in which the circumferential muscle fibers of the tubulatus muscle (referred to as the tubular *copulo-copularis* muscle by Fürbringer) produce peristaltic motions to force a turgid clavatus muscle (or the core *longitudinalis linguae* muscle using Fürbringer's terminology) anteriorly or posteriorly to bring about dental plate protraction or retraction. This mechanism is analogous to a simple technique by which one may thread a drawstring through the fold surrounding the aperture of a drawstring bag or hood of a sweater; if a large safety pin is attached to one end of the drawstring and is inserted into one hole in the apertural fold, then one can manipulate the material around the safety pin to cause the pin to emerge from the other hole. Because the dental plate is connected to the clavatus muscle by a tendon, any posterior movement of the clavatus muscle causes dental plate retraction. In Fürbringer's model, the contraction of the perpendicularis muscle causes the portion of the clavatus muscle that emerges from the posterior end of the tubulatus muscle to flare laterally and thus anchor the clavatus muscle by not allowing it to slide through the lumen of the tubulatus muscle. This mechanism is similar to a shoestring (analogous to the clavatus muscle and its tendon) with a stopper-knot tied on one end (analogous to the flared perpendicularis muscle). If one threads the free end through a drinking straw (analogous to the tubulatus muscle) the stopper knot will not allow the whole shoestring to be pulled through the drinking straw.

Luther (1938) developed a more detailed hypothesis of the retractor complex morphology by improving on Fürbringer's original anatomical description. Luther (1938) describes the clavatus muscle as a conical wedge that is inserted into the lumen of the tubulatus muscle such that the largest portion of the clavatus muscle projects from the posterior end of the tubulatus muscle. Luther (1938) agreed with Fürbringer's

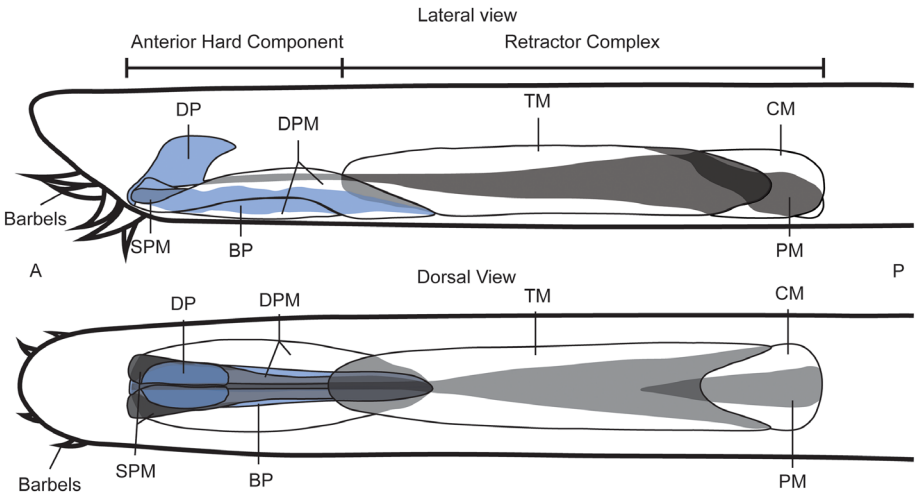

FIGURE 2 The morphology of the hagfish feeding apparatus in the Pacific hagfish from lateral and dorsal views. Cartilaginous elements are shaded in blue. Grey shading is using to indicate portions of tissue beneath softer tissue. Abbreviations: SPM, Superficial protractor muscles; DPM, Deep protractor muscles; TM, Tubulatus muscle; CM, Clavatus muscle; PM, Perpendicularis muscle; BP, Basal plate; DP, Dental plate. A = Anterior, P = Posterior

(1875) assertion that the flared posterior end of the clavatus muscle prevents it from sliding through the tubulatus muscle. This flaring effect was thought to be enhanced by the activation of perpendicularis muscle.

Dawson's (1963) analysis solidified HFA terminology and used Luther's (1938) anatomical descriptions to develop a new functional hypothesis (Figure 3b). In this "core-wedge" hypothesis, the wedge-shaped clavatus muscle "core" contracts longitudinally to generate most of the forces used in dental plate retraction. However, without antagonism, the posterior end of the contracting clavatus muscle would simply move closer to the dental plate. The antagonistic force is generated by the tubulatus muscle, which was thought to function as a structurally supportive, sheath-like spacer that resists the compression generated by the contraction of the clavatus muscle. Additionally, further extension of the tubulatus muscle could serve to passively extend the inactive clavatus muscle to its resting, precontracted length. Dawson (1963) also supports the theory that the perpendicularis muscle acts as an anchor by contracting to flare the posterior end of the clavatus muscle so that it cannot slide through the tubulatus muscle.

More recent research by Clark et al. (2010) supports Dawson's anatomical and functional descriptions of the retractor complex. Results from their electromyographical study show that the tubulatus, clavatus, and perpendicularis muscles simultaneously contract during dental plate retraction, but are all relaxed during protraction (Clark et al., 2010). This discovery enabled them to further hypothesize that the retractor complex is a muscular hydrostat that provides structural support while generating movement (Clark et al., 2010); similar in

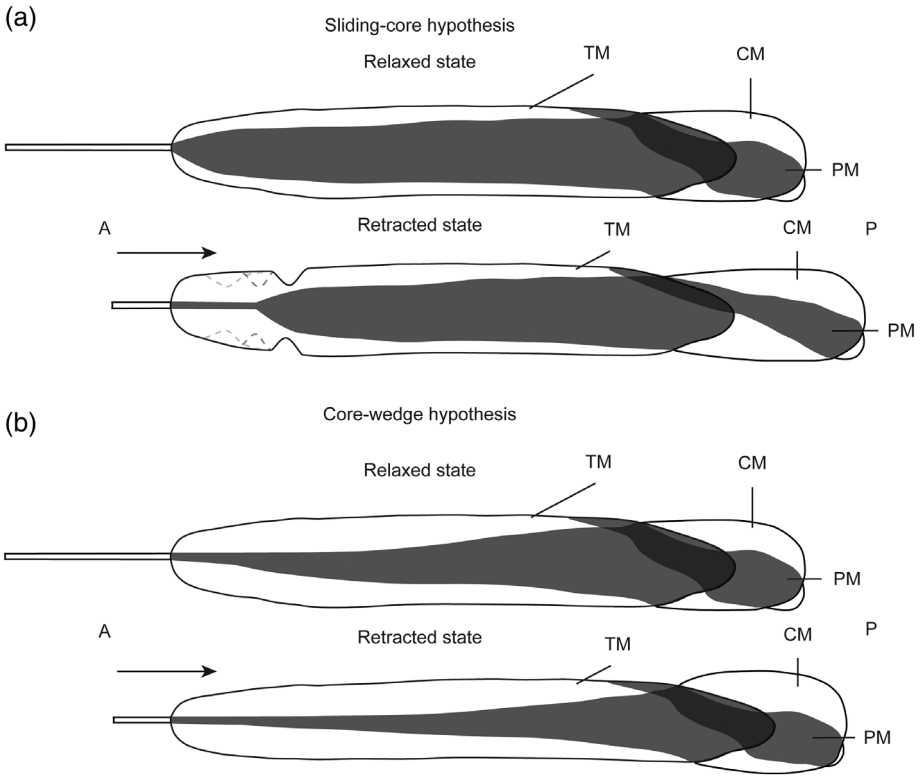

FIGURE 3 A comparison of feeding apparatus functional hypotheses. (a) Fürbringer's sliding-core hypothesis, by which peristaltic motions generated by the tubulatus muscle force a turgid cylindrical clavatus muscle core anteriorly or posteriorly resulting in dental plate protraction or retraction. (b) Dawson's core-wedge hypothesis: Contraction, and thus shortening of the clavatus core muscle, directly creates forces for dental plate retraction. The tubulatus muscle supports the clavatus muscle by contracting to act as a spacer, anchoring the posterior end of the clavatus muscle. In both hypotheses, the perpendicularis muscle fits in a bifurcation of the clavatus muscle and is suspected to contract to flare the posterior end of the clavatus muscle to prevent it from sliding through the tubulatus muscle. A = anterior, P = posterior

function to the buccal mass of cephalopod beaks (Uyeno & Clark, 2015; Uyeno & Kier, 2005; Uyeno & Kier, 2007).

In this study, we use serial histological data sets and surface scans to accurately describe the morphology and function of the retractor complex of the HFA by building 3D reconstructions that include detailed descriptions of muscle fiber orientation. We examined feeding apparatuses from specimens of Pacific Hagfish (*Eptatretus stoutii*) and Atlantic hagfish (*Myxine glutinosa*) because these species are regularly accessable to North American researchers and because each represents one of the two major lineages (subfamilies Myxininae and Eptatretinae) of hagfishes that account for approximately 90% of the 78 extant species (Fernholm et al., 2013). These 3D reconstructions and histological data sets, derived from detailed, cell-level anatomy that takes into consideration soft tissue fiber orientations, will enable us to evaluate the structure as a muscular hydrostat and test the core-wedge hypothesis.

2 | MATERIALS AND METHODS

2.1 | Specimens

Thirty-eight specimens of Pacific hagfish (*Eptatretus stoutii*, Lockington, 1878) and ten Atlantic hagfish (*Myxine glutinosa*, Linnaeus, 1758) were used in this study. Live specimens of *E. stoutii* were provided by the Washington Department of Fish and Wildlife and Olympic Coast Seafoods LLC (Port Angeles, WA). Four live specimens of *M. glutinosa* were provided by NOAA Fisheries and Cape Ann Seafood Exchange (Gloucester, MA). The remaining six specimens of *M. glutinosa* were collected at Shoals Marine Lab (Appledore Island, ME). All specimens were shipped to, and housed at, Valdosta State University (VSU).

Morphometric data were recorded from these specimens of *E. stoutii* (total length = 454.2 ± 59.9 mm and mass = 136.9 ± 42.6 g) and *M. glutinosa* (total length = 460.3 ± 40.1 mm and mass = 78.1 ± 21.3 g). Animals were housed in six 19 L buckets in an angled water table, which were part of a 227 L recirculating artificial saltwater system. Saltwater in the system was maintained at approximately 8 °C using a water chiller, and salt concentration was kept at approximately 34 ppt by adding distilled water to the system as water evaporated (Gustafson, 1935). The buckets were kept covered to reduce evaporation and to simulate a naturally dark habitat. Live specimens were fed once every 2 weeks with approximately 3 cm^3 pieces of chopped squid or mullet. Animal care, handling, and euthanization procedures were approved by Valdosta State University's Institutional Animal Care and Use Committee (VSU AUP-00070-2017).

2.2 | Dissection of feeding apparatuses

Specimens were euthanized using 400 mg MS222 (Finquel anaesthetic, Argent Chemicals, Redmond, WA) and 200 mg $NaHCO_3$ (pH buffer) mixed in 1 L of seawater. The anteromost portion of these hagfishes (approximately 30% of the total length) was then removed and immediately fixed in 10% neutral buffered formalin for 24 hr. For dissection, a circumferential incision (a) was made just beyond the posterior end of the HFA (Figure 4). This circumferential cut was expanded by making an anteriorly running incision (b) along the ventral side of the body, ending at the mouth (Figure 4). Once at the mouth, we made an oblique incision (c) to separate the skin covering the snout from the rest of the cranial skin (Figure 4). The skin was then peeled back to expose the HFA and its associated connective tissues. Using a blunt probe, the connective tissues connecting the HFA

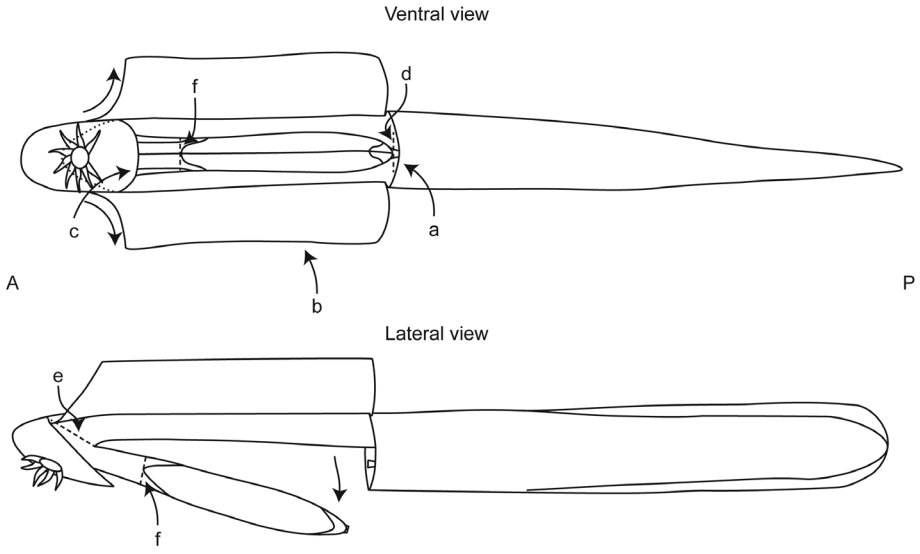

FIGURE 4 Ventral and lateral views of the methods used for excising the retractor complex of the hagfish feeding apparatus from specimens. (a) Indicates a circumferential incision just beyond the posterior end of the feeding apparatus. (b) Shows a ventral expansion of incision a in the anterior direction ending right before the mouth. (c) Indicates an oblique incision separating the skin of the snout from the rest of the hagfish's skin. (d) Represents cutting the connective tissues holding the posterior end of the feeding apparatus in place. (e) Represents cutting the notochord and body wall musculature to remove the snout and feeding apparatus from the body. (f) Represents bisecting the feeding apparatus at the anterior end of the tubulatus muscle. A = anterior, P = posterior

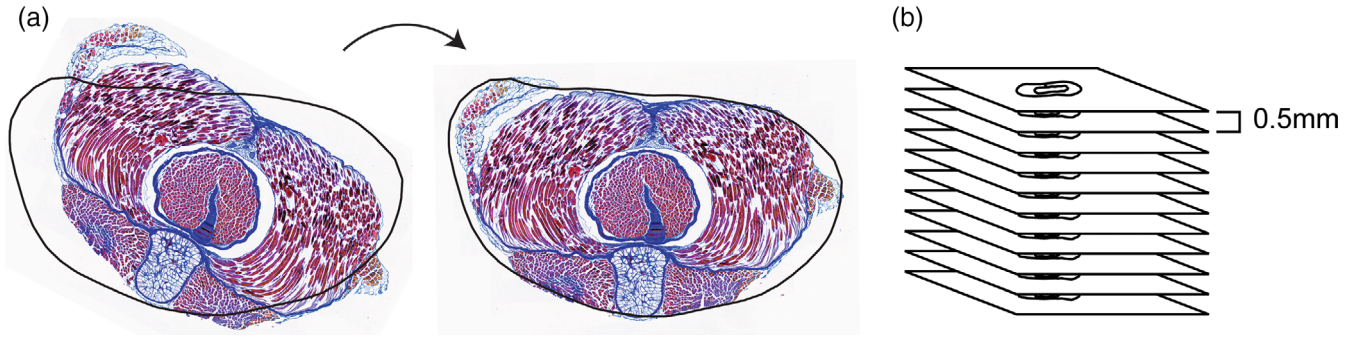

FIGURE 5 Methods for aligning section scans with contours generated by transecting HFA retractor complex surface meshes. (a) An example of how scans were visually aligned to contours. (b) The conversion of two dimensional .tif files into a 3D .NIfTI file format

to the ventral body wall were broken. The thick tissues connecting the posterior end of the HFA to the body wall were cut (d), leaving the HFA only attached to the anterior cranial structures near the mouth (Figure 4). The HFA and snout (the entire naris/mouth region) were then separated from the body (e) by cutting the notochord and body wall musculature along the oblique incision (Figure 4). The snout and hard anterior component were then removed (f) by bisecting the HFA at the anterior end of the tubulatus muscle (Figure 4). The remaining retractor complex was then three-dimensionally scanned at high resolution with an Artec Space Spider surface scanning system (Luxembourg City, Luxembourg) to generate surface meshes that were then used to generate a series of aligned contours. These contours allowed us to visually realign each digitized slice (Figure 5a-b) in order to create a more accurate, histology-based, three-dimensional reconstruction.

2.3 | Histological preparation

We followed standard paraffin histological protocols established by Kier (1992). The HFA retractor complexes were fixed for 48 hr in 10% neutral-buffered formalin (*M. glutinosa* specimens from Shoals Marine Lab were fixed for 24 hr, rather than 48, because they were euthanized and fixed for 24 hr prior to their arrival at VSU). After fixation, the tissue was cut into a series of 10 mm segments to facilitate efficient histological paraffin infiltration using cassettes. Orientation and sequence were carefully preserved to facilitate subsequent reconstructions. These tissue segments were then dehydrated in a series of ethanol baths. Tissue segments were run for 2 hr in each bath in the following sequence: (1) 15% ETOH; (2) 30% ETOH; (3) 45% ETOH; (4) 60% ETOH; (5) 75% ETOH; (6) 90% ETOH; and (7) 100% ETOH. Retractor complexes were then bathed for 2 hr in a 50% absolute ethanol and 50% citrisolv solution, followed by 2 hr in 100% citrisolv, to facilitate the infiltration of liquid paraffin during a series of three 1-hr paraffin baths under vacuum. Paraffin infiltrated chunks of tissue were then embedded into wax blocks for sectioning.

Wax blocks were cut and faced, and a Finesse ME+ Microtome (Waltham, MA) was used to cut 12 μm thick sections. Five sections were collected every 500 μm. Collected sections were placed in a 46 °C water bath for approximately 20 min to expand and remove cutting distortions. Sections were then placed on slides prepared with Mayer's albumin and heat fixed on a 43 °C hot plate overnight (Kier, 1992).

A modified Milligan's trichrome staining protocol (Kier, 1992) was used to differentiate between three tissue types; muscle tissue stained magenta, connective tissue appears blue, and blood cells stain orange. The staining process was carried out using a Thermo Scientific Gemini AS automated slide stainer (Waltham, MA). Cover slips were then affixed to the stained slides using permount (Fisher Chemical, Waltham, MA).

2.4 | Three-dimensional reconstruction

Whole sections were digitized using the Microvisioneer Manual Whole Slide Scanning software (microvisioneer.com, Josef Bauer, Freising, Germany). A plan10×/0.25 objective, paired with a Basler acA 1920-40uc high speed camera (Ahrensburg, Germany) attached to an Olympus BX microscope via an Olympus 1×/c-mount adapter, was used to produce images with a 0.59 μm per pixel resolution. Scanned cross-sectional images were aligned to their natural position by fitting them to contours generated by transecting the previously mentioned HFA retractor complex surface meshes every 500 μm (Figure 5a).

A custom MATLAB script was used to space the parallel, aligned .tif images in three-dimensions, each at 500 μm apart, in an open source volumetric .NIfTI file format (Figure 5b). These .NIfTI files were then imported into ITK-SNAP (Philadelphia, PA) for segmentation and to build the 3D reconstruction. Components that appeared in each image slice were identified and semiautomatically segmented with color coded labels. These label colors were used throughout the entire structure, allowing us to produce a 3D reconstruction of the retractor complexes of the HFA.

3 | RESULTS

Relative to body size, *E. stoutii* have significantly larger feeding apparatuses (0.22*TL* vs. 0.18*TL*), comprising larger hard and soft components (represented by BPL and RCL, respectively), than those recorded from *M. glutinosa* (Figure 6a,b). The retractor complex of the

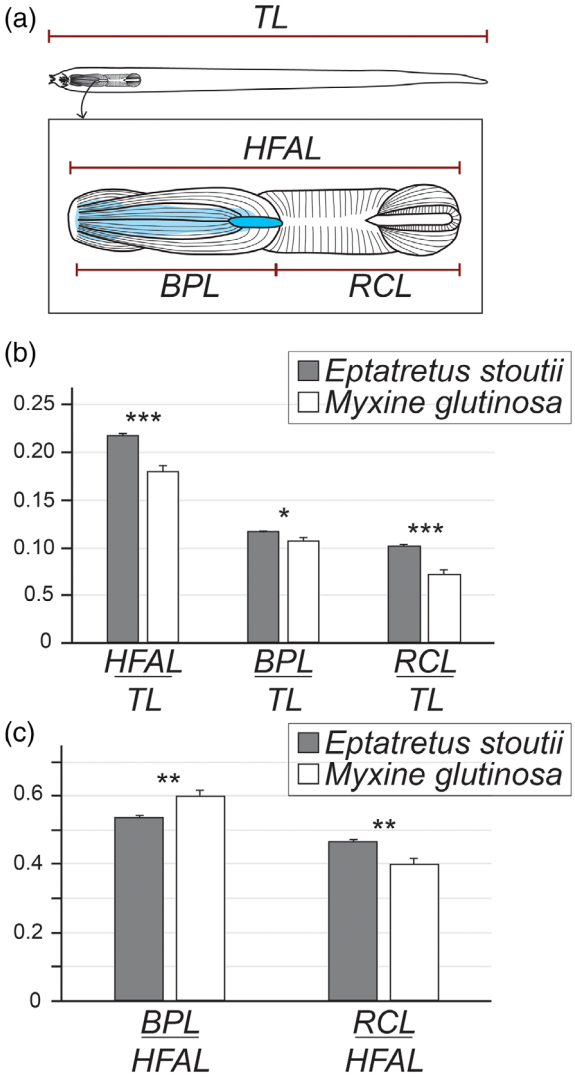

FIGURE 6 Morphometric data from the feeding apparatuses of *E. stoutii* and *M. glutinosa*. (a) Methods for measuring the total length (TL), feeding apparatus length (HFAL), basal plate length (BPL), and retractor complex length (RCL). (b) Mean lengths of the feeding apparatus, basal plate, and retractor complex as a percentage of the total length. (c) Mean lengths of the basal plate and retractor complex as a percentage of the feeding apparatus length. Error bars represent *SEM*. Significant differences between mean data are represented as * ($p < .05$), ** ($p < .005$), and *** ($p < .0005$)

HFA is shaped like a club, bearing a thin, cartilaginous, anterior end and a wider, muscular, posterior end (Figure 7). In both *E. stoutii* and *M. glutinosa*, the entire club-shaped structure is ensheathed by a thin connective tissue layer that is continuous with the anterior basal plate cartilage and with a posterior tendon that secures the HFA to the body wall musculature. Within this connective tissue sheath, the retractor complex of both species is composed of a similar vasiform tubulatus muscle bearing a central lumen (Figure 8a) that contains most of the conically shaped clavatus muscle (Figure 9a) and the anterior end of the wedge-shaped perpendicularis muscle (Figure 10a). The morphologies of the tubulatus, clavatus, and perpendicularis muscles are described below.

3.1 | Morphology of the Tubulatus muscle

The prominent tubulatus muscle spans the anterior 90% of the length of the retractor complex (Figure 7). Cross-sections at any point along the longitudinal axis of the tubulatus muscles of both species show that their entire circumferences are not formed of hoop-like muscle fibers. Instead, the tubulatus muscle is composed of semicircular (or semicurved) fibers spanning between ventral and dorsal connective tissue strips (Figure 8b.1–3). These ventral and dorsal connective tissue strips are continuous with a connective tissue sheath surrounding the entire retractor complex. Furthermore, the anterior portions of these strips anchor the tubulatus muscle to the basal plate cartilage (Figure 8c).

In addition to securing the position of the tubulatus muscle relative to other muscles in the retractor complex, the ventral and dorsal connective tissue strips also connect the muscular left and right lateral walls of the tube to each other (Figure 8b.1–3). The muscle fibers that form these lateral walls originate along the ventral connective tissue strip and insert on the dorsal connective tissue strip, following a path parallel to the curving surface of the tube (Figure 8b.1–3). In transverse sections, the muscle fibers that form the lateral walls appear obliquely cut (Figure 8d). Parasagittal sections confirm that these muscle fibers are not perpendicular to the longitudinal axis of the muscle, but instead, are oriented posterodorsally from their origin with a pennation angle of approximately 108.5° in the measured *E. stoutii* specimen and 106.4° in the measured *M. glutinosa* specimen. Posteriorly, the lateral walls of the tubulatus muscle extend beyond the dorsal and ventral connective tissue strips, forming left, and right flap-like extensions. Thus, the posterior end of the tubulatus has a notched appearance (Figure 8a).

3.2 | Morphology of the Clavatus muscle

The clavatus muscle spans the entire length of the retractor complex and superficially resembles a darning needle (Figure 9). At the thin anterior end, the clavatus muscle transitions into a long, narrow tendon (Figure 9b) that exits the anterior end of the retractor complex and runs along a groove in the dorsal surface of the basal plate to insert medially on the posterior edge of the dental plate. This tendon is formed by the fusion of several longitudinally twisting connective tissue ribbons that can be seen in cross-sections dispersed amongst muscle fibers throughout the anterior half of the clavatus muscle (Figure 9b). Muscle fibers originate on this tendon and orient posteriorly, nearly parallel to the long axis of the retractor complex (Figure 9c). At approximately one third of its length, the clavatus muscle bifurcates into left and right rami (Figure 9a). Within the tubulatus muscle, the rami of the clavatus muscle remain tightly pressed together such that their fibers assume a longitudinal orientation.

The posterior quarter of the clavatus muscle emerges from the lumen of the tubulatus muscle to form the terminal bulb of the retractor complex (Figure 9d.2–4). As such, the clavatus muscle rami diverge laterally to form the "eye" of the darning needle: a dorsoventrally oriented space occupied by the perpendicularis muscle. Muscle fibers

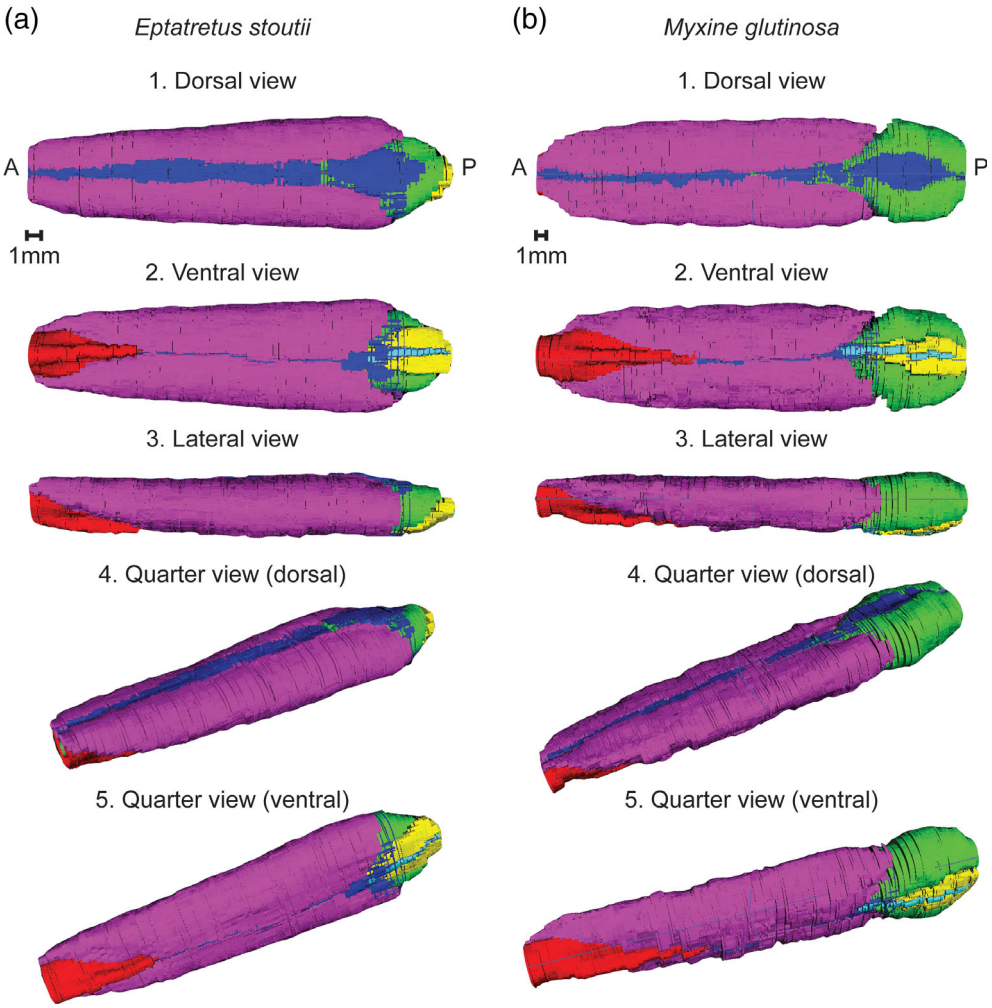

FIGURE 7 Three-dimensional reconstructions of the retractor complex of *E. stoutii* (a) and *M. glutinosa* (b). 1) Similar dorsal views of a complete reconstruction of the retractor complex. 2) Similar ventral views of a complete reconstruction of the retractor complex. 3) Similar lateral views of a complete reconstruction of the retractor complex. 4) Similar quarter views (dorsal) of a complete reconstruction of the retractor complex. 5) Similar quarter views (ventral) of a complete reconstruction of the retractor complex. Here: The tubulatus muscle is shown in purple; the clavatus muscle in green; the perpendicularis muscle in yellow; the basal plate in red; connective tissue strips in dark blue; and the perpendicularis cartilage in light blue. Reconstructions are shown at a similar scale to enable comparison between species. A = Anterior, P = Posterior

within the rami of the clavatus muscle follow the lateral contours of, and extend beyond, the perpendicularis muscle (Figure 9d). The rami of the clavatus muscle curve around the posterior edge of the perpendicularis muscle and insert on each other, thereby completing a structure that resembles the "eye" of a needle. The heads of the rami are fused with each other by the continuity of the connective tissue sheathes on the left and right rami at the posterior surface of the terminal bulb of the HFA. Also at this location, these connective tissue sheaths become continuous with the connective tissue layer ensheathing the entire retractor complex.

3.3 | Morphology of the Perpendicularis muscle

The perpendicularis muscle occurs within the posterior quarter of the retractor complex where it is positioned between the left and right rami of the clavatus muscle (within the darning needle's "eye"; Figure 7). In order to fit within this lumen, the perpendicularis muscle has the general shape of an obliquely oriented, laterally flattened, elliptical cylinder, in which the oval bases are flush with the dorsal and ventral surfaces of the surrounding clavatus muscle. As such, the muscle appears to be oriented obliquely to the long axis of the retractor complex. The dorsal surface is anchored anteriorly to the dorsal connective tissue strip of the tubulatus muscle, and the ventral surface inserts posteriorly to the perpendicularis cartilage and the connective tissue sheath surrounding the retractor complex (Figure 10b,c).

At its anterior end, the cross-sectional profile of the perpendicularis muscle is wedge-shaped (Figure 10b.1) with a blunt dorsal end and a narrow ventral end. In this region the perpendicularis muscle is composed of obliquely oriented (anterodorsal to posteroventral) muscle fibers (Figure 10b.1,c). Subsequent sections show the ventral end of the perpendicularis muscle projecting and inserting medially on the perpendicularis cartilage, a small cartilaginous bar that serves to anchor the muscle to the connective tissue sheath surrounding the retractor complex (Figure 10b.2,c). This feature occurs in specimens of both *E. stoutii* and *M. glutinosa*, at approximately 1 mm posterior to the anterior end of the perpendicularis muscle. Here, a lateral flaring of the ventral portion of the perpendicularis muscle results in a pear-shaped cross-sectional profile (Figure 10b.3). Sections taken from this area show muscle fibers in the most ventral region of the perpendicularis muscle leaving their oblique orientation and progressively becoming closer to parallel with the long axis of the retractor complex (Figure 10b.2–4,c). Between the point at which the perpendicularis muscle inserts on the perpendicularis cartilage and the point at which it exits the lumen of the tubulatus muscle, muscle

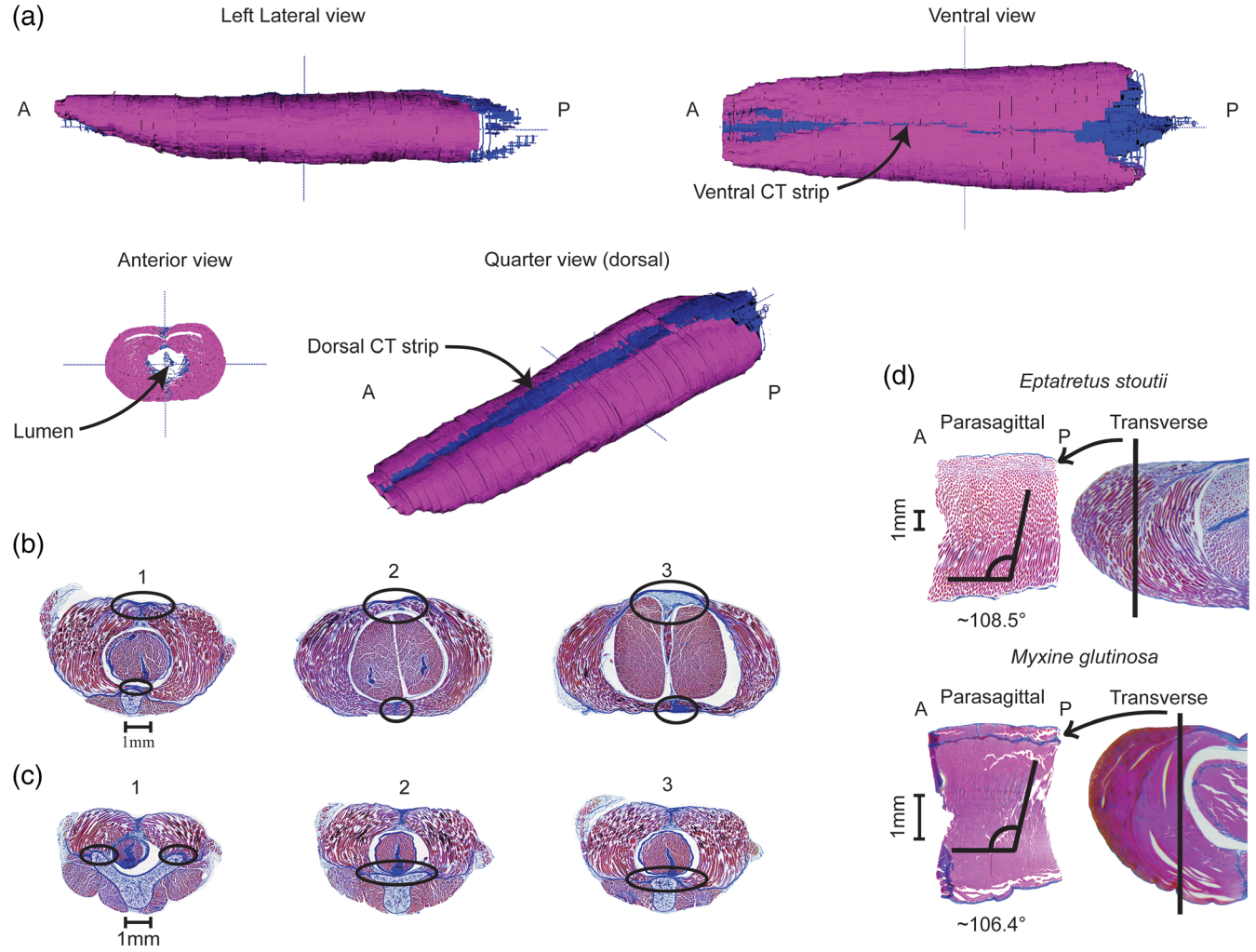

FIGURE 8 A reconstruction of the tubulatus muscle of an *E. stoutii* specimen alongside sections that illustrate significant histological features and a comparison of *E. stoutii* and *M. glutinosa* tubulatus muscle fiber orientations. (a) A complete reconstruction of the tubulatus muscle of an *E. stoutii* specimen in lateral, ventral, anterior and quarter views. (b) A series of transverse sections show dorsal and ventral connective tissue strips forming the mid-ventral and mid-dorsal walls of the vasiform tubulatus muscle in an *E. stoutii* specimen. These strips serve to connect the muscular, left and right lateral walls as well as secure the position of the tubulatus relative to the other muscles. 1–3 are sections from approximately 25%, 49%, and 75% of the length of the retractor complex respectively. (c) A series of transverse sections that show the attachment of the anterior end of the tubulatus muscle to the basal plate in an *E. stoutii* specimen. 1–3 are sections from approximately 6%, 12%, and 18% of the length of the retractor complex, respectively. (d) Parasagittal sections (left) from the section planes indicated by the lines in transverse sections (right) from the tubulatus muscles of a specimen of *E. stoutii* and *M. glutinosa*. The transverse sections show obliquely cut muscle fibers following a path parallel to the curving surface of the tube. Parasagittal sections show the posterodorsal orientation of muscle fibers comprising the lateral walls of the tubulatus muscle. Relaxed tubulatus muscle fiber orientation angles were measured for both *E. stoutii* and *M. glutinosa*. A = anterior, P = posterior

fibers assume an angle more parallel to the long axis of the retractor complex (Figure 10b.2–4,c). As the perpendicularis muscle exits the posterior end of the lumen of the tubulatus muscle it is almost entirley composed of muscle fibers oriented nearly parallel to the long axis of the retractor complex (Figure 10b.3–4,c). This shift in muscle fiber orientation marks the point at which the perpendicularis muscle emerges ventrally from between the rami of the clavatus muscle. Posterior to this emergence, the perpendicularis muscle is decoupled from the dorsal connective tissue strip of the tubulatus muscle (Figure 10b.4). From the point at which the perpendicularis muscle emerges from between the clavatus rami to its posterior end, the whole muscle tapers to form a rounded tip that makes up the posteroventral border of the retractor complex (Figure 10b.5,c).

4 | DISCUSSION

This research described the retractor muscle complex of the HFA from two dominant lineages of the Myxinindae: the Eptatretine *E. stoutii* and the Myxinine *M. glutinosa*. Detailed histological analyses coupled with 3D reconstructions were performed to provide a novel characterization of their retractor complexes at the level of muscle

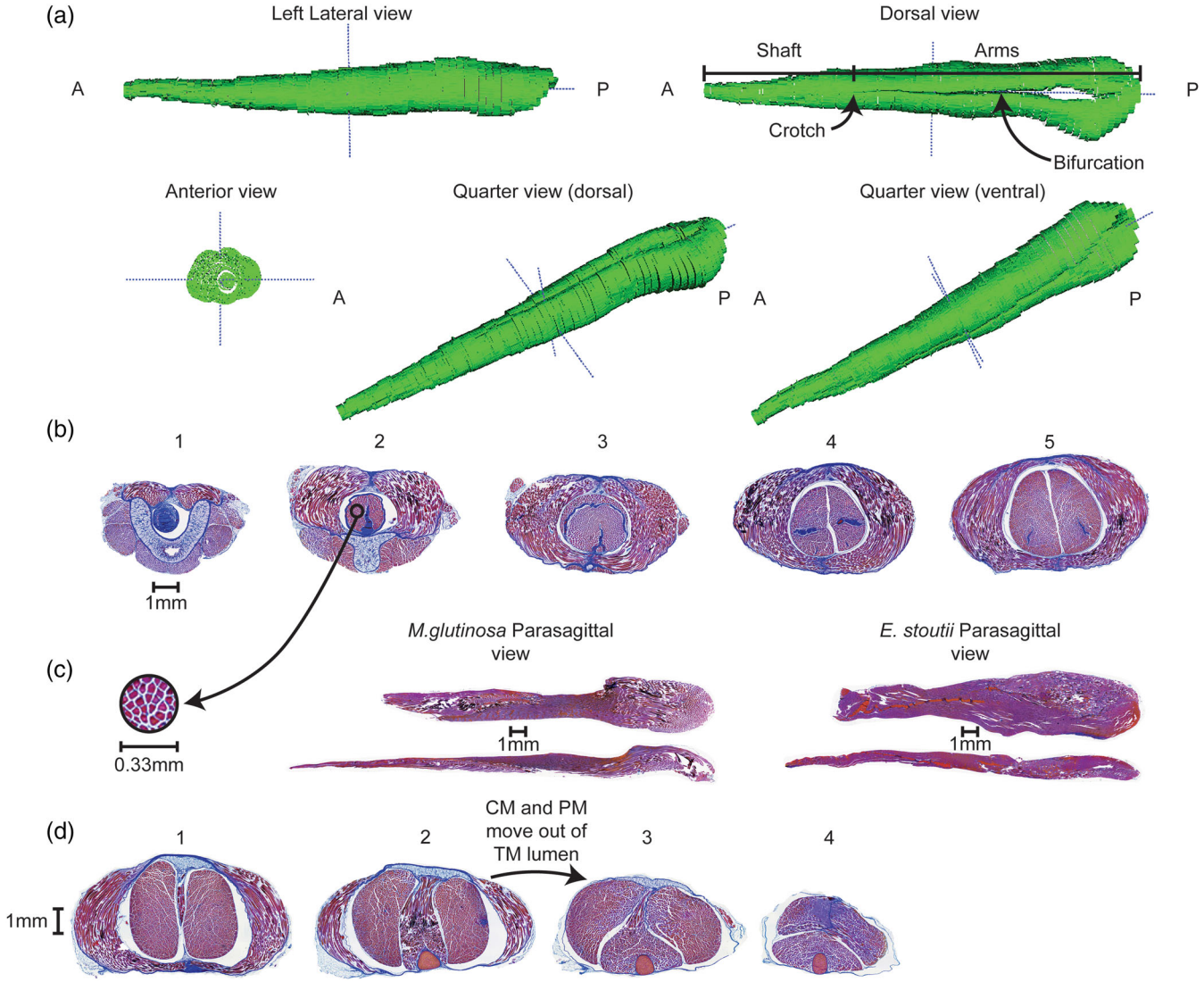

FIGURE 9 A reconstruction of the clavatus muscle of an *E. stoutii* specimen alongside sections that illustrate significant histological features and a comparison of *E. stoutii* and *M. glutinosa* clavatus muscle structural differences. (a) A complete reconstruction of the clavatus muscle of an *E. stoutii* specimen in lateral, ventral, anterior, and two quarter views. (b) A series of transverse sections from the anterior end of the retractor complex of an *E. stoutii* specimen that show details of how the dental plate tendon inserts onto the clavatus muscle. 1–5 are sections from approximately 0%, 12%, 26%, 40%, and 52% of the length of the clavatus muscle respectively. (c) Transverse and parasagittal cross-sectional evidence of the nearly longitudinal orientation of muscle fibers comprising the clavatus muscles of a *M. glutinosa* and *E. stoutii* specimen. (d) A series of transverse sections from an *E. stoutii* specimen that show the rami of the clavatus muscle becoming distinctly separated by the perpendicularis muscle and exiting the lumen of the tubulatus muscle. 1–5 are sections from approximately 75%, 82%, 88%, and 94% of the length of the clavatus muscle, respectively. A = anterior, P = posterior

and connective tissue fiber orientations. Our histological analyses suggest that the retractor complex functions as a muscular hydrostat, which advances a new functional hypothesis of dental plate retraction. These functional hypotheses apply to both species examined despite significant interspecific differences in the size of the HFA.

4.1 | The HFA retractor complex as a muscular hydrostat

Our fine-scale morphological analysis of the HFA retractor complex suggested that it functions as a muscular hydrostat, which corroborates the assertions of Clark et al. (2010) and Uyeno and Clark (2015). Muscular hydrostats are 3D blocks of muscle that are composed of multiple orientations of muscle fibers and are capable of generating both forceful deformations used in movement, as well as creating turgidity that provides structural support (Kier & Smith, 1985). This seems to be the case with the HFA retractor complex, as previous studies show that it is capable of generating strong force for the retraction of the dental plate cartilage in addition to forming a stiff structural support element for the basal plate cartilage (Clark et al., 2010; Clark & Summers, 2007; Clark & Summers, 2012; Uyeno & Clark, 2015). However, because of the lack of fiber organizational

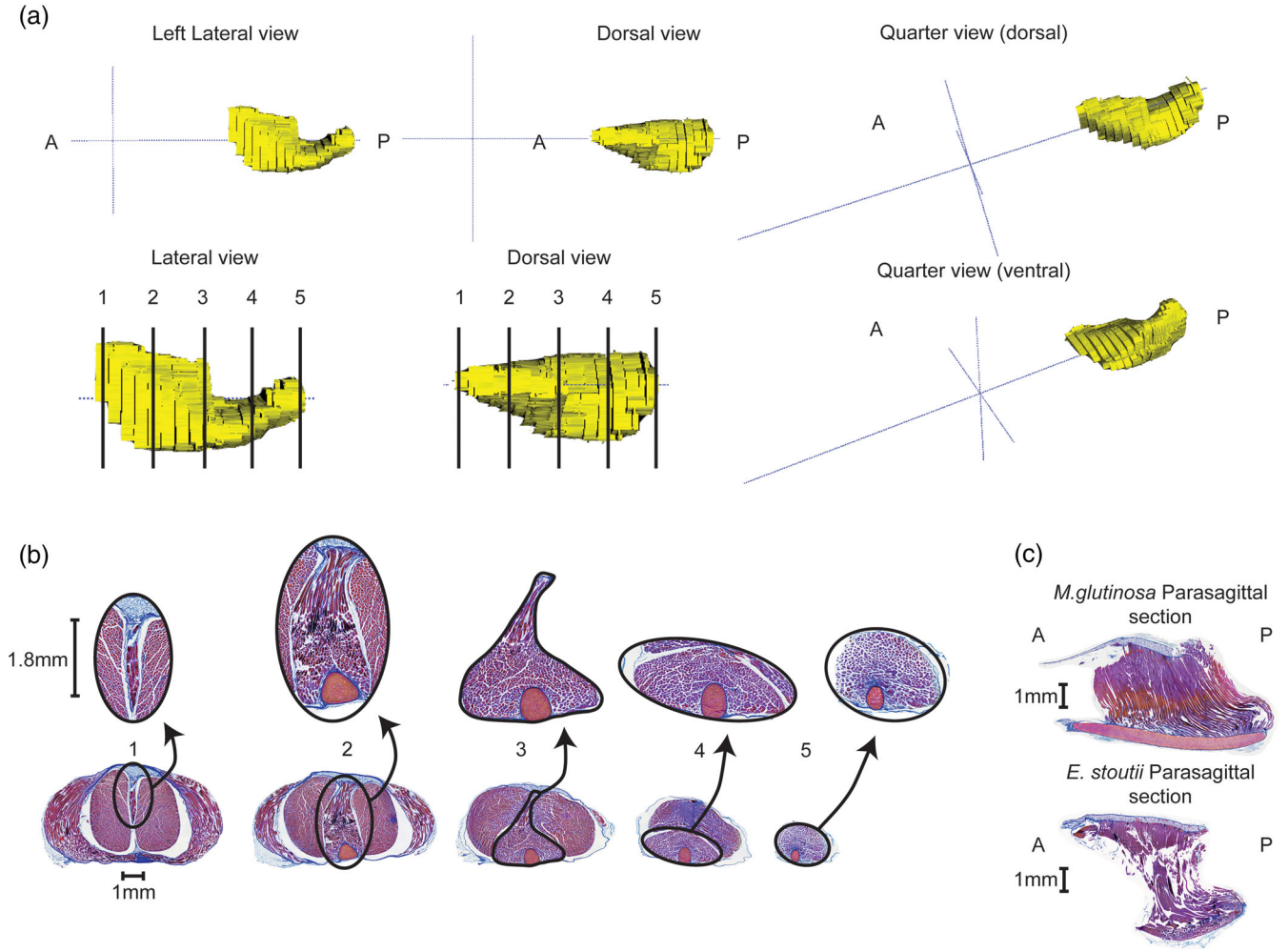

FIGURE 10 A reconstruction of the perpendicularis muscle of an *E. stoutii* specimen alongside sections that illustrate significant histological features and a comparison of *E. stoutii* and *M. glutinosa* perpendicularis muscle fiber orientations. (a) A complete reconstruction of the perpendicularis muscle of an *E. stoutii* specimen in lateral, ventral, and two quarter views. Additionally, a lateral and dorsal view have been magnified and marked to illustrate the planes from which sections (shown in b) were taken to demonstrate the change in location and orientation of muscle fibers. (b) Transverse sections of the perpendicularis muscle of an *E. stoutii* specimen, taken at five (1–5) locations, that show the change in cross-sectional profile and fiber orientations found throughout the muscle. (b.1) A transverse section showing the anterior end of the perpendicularis muscle which has a wedge-shaped profile and is comprised of obliquely (anterodorsal to posteroventral) oriented muscle fibers. (b.2) A transverse section showing the ventral extension and lateral expansion of the cross-sectional profile of the perpendicularis muscle. Here, one can observe the transition from obliquely oriented muscle fibers to longitudinally oriented ones. Additionally, one can also observe the perpendicularis muscle attached to the perpendicularis cartilage. (b.3) A transverse section showing the pear-shaped profile of the perpendicularis muscle as it exits the lumen of the tubulatus muscle. Here, the perpendicularis muscle is almost completely comprised of longitudinally oriented muscle fibers. (b.4) A transverse section showing the perpendicularis muscle removed from between the rami of the clavatus muscle. (b.5) A transverse section from the posterior end of the retractor complex showing the tapering end of the perpendicularis muscle. (c) Parasagittal sections of the perpendicularis muscle, in a *M. glutinosa* and *E. stoutii* specimen, showing the change in muscle fiber orientations. A = anterior, P = posterior

detail that differentiate between muscle and connective tissue, previous anatomical studies (Cole, 1907; Dawson, 1963; Fürbringer, 1875; Luther, 1938) did not consider the function of the retractor complex muscles (the tubulatus, clavatus, and perpendicularis muscles), and the associated connective tissue sheathes and tendons as a muscular hydrostat. Additionally, a detail that further masked the diagnosis of the HFA retractor complex as a muscular hydrostat is that none of these muscles contain multiple fiber orientations (Figures 8–10).

The muscle fibers within each muscle are uniform in orientation; however, the retractor complex as a whole has antagonistic fiber orientations and likely functions as a muscular hydrostat (Figures 8–10). Thus, simultaneous contractions of the tubulatus, clavatus, or perpendicularis muscles in various combinations likely generate skeletal support or motive force for dental plate retraction. Because each muscle fits together, the contribution of connective tissue sheathes that surround and, in places, connects these muscles becomes important

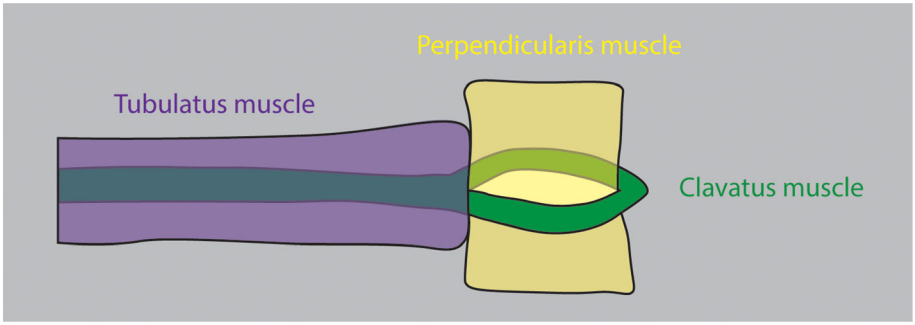

FIGURE 11 An illustration of the perpendicularis muscle acting as a cotter pin. Because the perpendicularus muscle is positioned between the "eye" of the clavatus muscle it effectively prevents the terminal bulb of the retractor complex from slipping into the lumen of the tubulatus muscle

to the overall muscular hydrostat. The connective tissue sheathes limit deformations, maintain the relative spatial relationships of the muscles, and may also control the tribological relationship of the clavatus muscle shaft sliding within the tubulatus muscle.

4.2 | Functional implications of the muscle fiber organizations in the HFA retractor complex

We hypothesized that the tubulatus muscle has dual purposes: to form a compression resistant spacer between the basal plate and the origin of the clavatus muscle (the terminal bulb), and also to generate force of retraction by elongating and increasing the distance between these two points (Figure 12). These functions depend on the organization of the tubulatus muscle as a novel "tubular bi-pennate" muscle. This term is used because the tubulatus muscle is formed of two muscular halves that are joined dorsally and ventrally by parallel connective tissue strips (Figure 8b). This muscle is described as bipennate because the origin and insertions of the semicircular fibers bear a pennation angle that differs from 90° (Figure 8d). As with planar bipennate muscles, this muscle fiber architecture is force optimized because it allows for an increased physiological cross-sectional area at the cost of shorter excursion (Gans, 1974; Powell, Roy, Kanim, Bello, & Edgerton, 1984). Thus, we hypothesized that activation of the tubulatus muscle results in: (a) a decrease in cross-sectional area perpendicular to its long axis (Figure 12), (b) a forceful concomitant lengthening that pushes the terminal bulb the HFA retractor complex posteriorly (Figure 12), followed by (c) a shearing motion due to the muscle fiber pennation angle that minimizes the distance between the posteriormost mid-dorsal point and the anteriormost mid-ventral point, resulting in the posterior bulb becoming angled dorsally (Figure 12).

Tension generated by both the tubulatus and clavatus muscles is transmitted to the dental plate tendon and results in dental plate retraction (Figure 12). Transmission of this force from clavatus muscle to dental plate tendon is supported by the twisting tendon/muscle interface, which may occur to increase surface area and strength of attachment (Figure 9b). The tension generated by the longitudinally oriented muscle fibers in the shaft of the clavatus muscle can be transmitted to the tendon because the posterior origin of the clavatus muscle is anchored within the terminal bulb. However, as the terminal bulb is firmly attached to the posterior end of the tubulatus muscle, previous hypotheses have assigned this muscle the role of a compression resistant spacer that provides separation between the terminal bulb and the basal plate in order to provide structural support for the contracting clavatus muscle. While function as a spacer is supported by our anatomical description, we hypothesize that the lengthening capacity of the tubulatus muscle plays a more significant role in dental plate retraction than previously thought (Figure 12). Indeed, the tubulatus muscle may play a larger role than the clavatus muscle itself; a post hoc comparison of the physiological cross-sectional areas of the tubulatus and clavatus muscles, measured in the specimens from which we sectioned for reconstructions, showed that the tubulatus muscle had approximately 7.5 times greater cross-sectional area than that the clavatus muscle in *E. stoutii*. This value

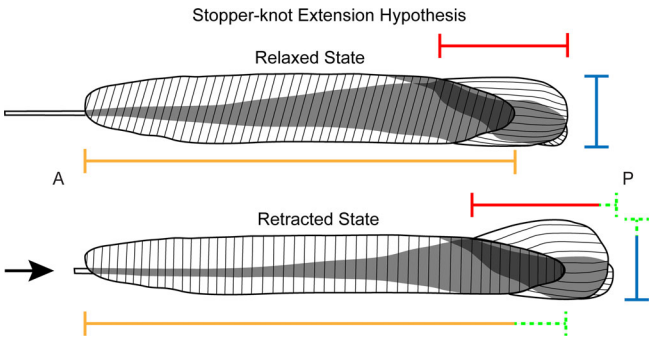

FIGURE 12 An illustration showing features of the "stopper-knot extension" hypothesis. Tubulatus muscle length is shown in yellow, retractor bulb length in red, and retractor bulb height in blue. Green dashed lines indicate dimensional expansion in the retracted state. The HFA retractor complex is shown in relaxed (top) and retracted (bottom) states. Note that in the relaxed state: (1) the muscle fibers comprising the tubulatus muscle show a posteriorly leaning pennation angle (shown here at 107°, which is the average pennation angle found in this study); (2) a larger percentage of the longitudinal muscle fibers of the clavatus muscle are found within the lumen of the tubulatus; (3) the perpendicularis muscle is obliquely oriented (anterodorsal to posteroventral); and (4) the terminal bulb is relaxed. In the retracted state: (1) the muscle fibers comprising the tubulatus muscle are realigned closer to perpendicular to the long-axis of the retractor complex, which results in a shear in the overall muscle profile; (2) the clavatus muscle is in a contracted state, with more of the muscle fibers being located near its posterior end; (3) the orientation of the perpendicularis muscle has shifted closer to the long-axis of the retractor complex; (4) the perpendicularis, in its contracted state, becomes shorter longitudinally and dorsoventrally; and (5) the terminal bulb is flared, and pushed dorsally by the shearing action of the tubulatus muscle. A = anterior, P = posterior

was 3.9 in *M. glutinosa*, suggesting that this species generates less forceful retractions. We also noted a significantly smaller relative size of the whole feeding apparatus in Atlantic hagfish, which was also reported by Clark and Summers (2007). Though the dental plate kinematics appear conserved across populations (Clark & Summers, 2007), the larger size of the whole feeding apparatus in *E. stoutii* musculature suggests that this species is capable of generating more forceful retractions of the tooth plates. Regardless of these discrepancies, the tubulatus muscle is potentially able to generate more force than the clavatus muscle in both species.

To the authors' knowledge, there is no correlation between HFA size and natural diet across different species of hagfishes. Clear differences in natural diets have not been identified between the two species studied, however, there have been more observations on the feeding behaviors in wild *M. glutinosa* (Auster & Barber, 2006; Cole, 1913; Gustafson, 1935; Leigh, Sparks, & Bemis, 2016; Pace, Mussi, Miragliuolo, Vivaldi, & Ardizzone, 2016; Shelton, 1978; Strahan, 1963) than in wild *E. stoutii* (Johnson, 1994; Worthington, 1905). Hagfishes generally feed on a variety of vertebrates and invertebrates (Martini, 1998) and use a variety of feeding modes (Glover & Bucking, 2015), which include opportunistic scavenging (e.g., Smith & Baco, 2003), predation (e.g., Zintzen et al., 2011), encounter competition (e.g., Auster & Barber, 2006), and passive transport of dissolved organic matter through their gills and skin (e.g., Glover, Bucking, & Wood, 2011). Among these fascinating feeding methods of hagfishes is their extraordinary ability to render ingestible morsels from extremely oversized prey. The HFAs of both *M. glutinosa* and *E. stoutii* are functionally capable of handling the tissues of baleen whale carcasses, as whale falls are a known source of for other species of *Eptatretus* and *Myxine* (Smith & Baco, 2003). Incidentally, a specimen of *Myxine glutinosa* has recently been observed anchoring itself to the blowhole of a live specimen of bottlenose dolphin (Pace et al., 2016).

We characterized the tubulatus muscle as a tubular bipennate muscle rather than as a tubular muscle invested with hoop-wise muscle fibers as reported in previous studies (Cole, 1907; Dawson, 1963; Fürbringer, 1875; Luther, 1938). Furthermore, we identified that the muscle fibers comprising the lateral walls bear a posteriorly oriented pennation angle in specimens of both *E. stoutii* and *M. glutinosa* (Figure 8d). We hypothesized that, when activated, these semicircular muscle fibers contribute to a series of deformations: (a) the size of the internal lumen is reduced and the shaft of the clavatus muscle is compressed; (b) the length of the tubulatus muscle increases until further extension is limited by the dorsal and ventral connective tissue strips and surrounding connective tissue sheath (Figure 12); (c) as with other pennate fibered muscles the angle of the fibers orient to become more perpendicular to the long axis of the retractor complex (Figure 12). Because the posterior end of the retractor complex is loosely attached within the hagfish body, this shift in muscle fiber orientation likely results in a shearing deformation of the tubulatus muscle, pulling together its anteroventral and posterodorsal ends as the whole muscle extends (Figure 12). Furthermore, another possible ramification of the bipennate muscle fiber organization of the tubulatus muscle is that, when contracting, the tubulatus will have a tendency to retract the basal plate, which in turn may facilitate dental plate retraction. This hypothesis is corroborated by electromyography data gathered by Clark et al. (2010).

The function of the clavatus muscle proposed here changes little from previous analyses (Clark et al., 2010; Clark & Summers, 2007; Clark & Summers, 2012; Cole, 1907; Dawson, 1963; Fürbringer, 1875; Luther, 1938; Uyeno & Clark, 2015); measurement of muscle fiber angles, relative to the long axis, in histological sections from *E. stoutii* and *M. glutinosa* specimens, show that the muscle fibers along the clavatus muscle shaft are oriented nearly longitudinally, and thus likely create direct tension in the dental plate tendon (Figure 9c). However, close investigation of fiber organization in the posterior portion of the clavatus muscle shows a novel anchoring mechanism (Figure 8c,d). Within this posterior terminal bulb, the perpendicularis muscle is fixed within the eye formed of the left and right rami of the clavatus muscle. (Figure 9c). As it extends through the eye, the perpendicularis muscle may function like a cotter pin to fix the posterior end of the clavatus muscle in position relative to the posterior end of the tubulatus muscle (Figure 11). The perpendicularis muscle has two attributes that facilitate such action. First, its position is fixed relative to the posterior end of the tubulatus muscle because the dorsal edge of the perpendicularis muscle originates on the dorsal connective tissue seam of the tubulatus muscle (Figure 10b,c). Likewise, the ventral edge of the perpendicularis muscle inserts on the perpendicularis cartilage embedded within the connective tissue sheath just posterior to the ventral connective tissue seam of the tubulatus muscle (Figure 10b,c). Second, activation of the perpendicularis muscle fibers may result in its lateral expansion due to the shortening of its dorsoventrally oriented fibers (Figure 10c). This prevents the terminal bulb from slipping into the lumen of the tubulatus muscle because activation of the perpendicularis muscle causes a lateral expansion resulting in the flaring of the terminal bulb.

4.3 | The "stopper-knot extension" hypothesis

In the past, the most accepted model of hagfish dental plate retraction was the "core-wedge" hypothesis (Clark et al., 2010; Dawson, 1963; Uyeno & Clark, 2015). Under this model, the posteriorly anchored clavatus muscle core contracts and shortens, resulting in dental plate retraction. While we postulated that contraction of the tubulatus muscle could be forceful, and may push the clavatus posteriorly, the muscle and connective fiber orientations found in the tubulatus muscle and terminal bulb suggest that other forces may play significant and hitherto unrecognized roles.

In the "stopper-knot extension" hypothesis the terminal bulb forms a swelling stopper-knot that is resistant to being pulled through the sleeve-like tubulatus muscle (Figure 12). The stopper knot swells because the needle-eye forming lateral rami of the clavatus muscle and the cotterpin-like perpendicularis muscle that they surround are mutually perpendicular and contract to flare laterally (Figure 12). Furthermore, the tubulatus muscle is capable of extending and thus pushing the stopper-knot terminal bulb away from the basal plate that anchors its anterior end (Figure 12). The process of retraction begins as the tubulatus muscle forcefully lengthens along the longitudinal axis. This

occurs because activation of the muscle fibers comprising the tubulatus muscle likely serve to reduce its diameter. As the tubulatus muscle lengthens, the terminal bulb of the retractor complex may be forcefully pushed posteriorly over the short distance allowed by the dorsal and ventral connective tissue strips (Figure 12). As the posterior extension of the tubulatus muscle becomes limited by its connective tissue sheath and by antagonistic action of the clavatus muscle, it may become a turgid spacer and capable of resisting compression generated by further clavatus muscle contraction (Figure 12). Additionally, because of the pennation angle of the tubular bipennate fiber arrangement of the tubulatus muscle, shearing occurs along the midsagittal plane that may result in the terminal bulb being tipped up dorsally and out of the longitudinal axis of the tubulatus muscle. This may be important in further enhancing the terminal bulb's function as a stopper-knot.

The HFA retractor complex is a muscular hydrostat that both produces the force of dental plate retraction as well as providing the structural hydrostatic support for the basal plate and the retractile force generators. The muscle fibers that may be generating retractile force belong to two distinct muscles: the clavatus and the tubulatus muscles. It is important to note that the clavatus muscle is organized as a parallel-fibered muscle that may allow for a great range of contractile lengths at the expense of peak force production. Likewise, the tubular bipennate muscle may benefit from a larger physiological cross-sectional area, and therefore, may be able to generate greater force over a smaller excursion. While all the physiological ramifications of pairing a force optimized muscle in series with a length optimized muscle are not considered here, it may be that this is a flexible system that can modulate or select between more forceful bites and wider gapes during feeding.

4.4 | Future directions

Our goal was to investigate the muscle fiber arrangements of the components that form the HFA retractor complex. Our analysis of this structure as a muscular hydrostat has produced a number of testable functional postulates. While our crude and preliminary electromyostimulation experiments using freshly euthanized specimens did not disprove our functional hypotheses, these postulates should be more formally explored. Hagfish are hearty organisms that can be maintained for over a year in captivity, however, they can be difficult to work with in the lab. This is because they lend themselves to rather short-lived physiological preparations and their extreme flexibility confounds the wide use of in-dwelling in situ physiology electrodes. However, with recent improvements in hyperflexible electrodes (Zhu et al., 2012) and miniaturized data telemetry (Cesarovic, Jirkof, Rettich, & Arras, 2011), sonomicrometry and longer-term electromyography studies may soon become possible. Currently, the most promising methods may be those that are capable of measuring or imaging deformation in hagfish during in vivo behaviors. One such approach may include the use of implantable radio-opaque markers in conjunction with x-ray reconstruction of moving morphology (XROMM; Orsbon, Gidmark, & Ross, 2018). This may be particularly useful if high-resolution specimen specific anatomy can be collected following experimentation. While hagfish bodies have very little differences in X-ray density, new techniques, such as diffusible iodine-based contrast-enhanced computed tomography (diceCT; Gignac & Kley, 2014) may allow us to distinguish between markers, muscle, connective tissue, sinuses, and skin. Mapping these anatomical features to behaviors described by the digitized movements of radio-opaque markers in 3D space may give us a realistic visualization of HFA function. Finally, while we selected two species that represent the two major subfamilies of hagfish, broadening the comparative aspect of the study to describe a more diverse array of hagfish species may be important to better understand the relationship between HFA biomechanics and their natural feeding behaviors and ecology.

The retractor complex of the HFA represents a novel mechanism constructed of compliant materials. The tubular bipennate muscle arrangement of the tubulatus muscle, in conjunction with the flaring cotter pin construction of the terminal bulb, allows the HFA to “bite” with surprising force and efficiency (Clark et al., 2010; Clark & Summers, 2007; Clark & Summers, 2012). Iida and Laschi (2011) note that animal bodies tend to take advantage of soft, elastic and flexible biomaterials to survive in complex unstructured environments. Thus, it is not surprising that mechanical engineers are investigating novel biological designs and control strategies for inspiration to develop novel robotics solutions at an ever-increasing pace (Rus & Tolley, 2015). The HFA retractor complex may serve as the basis of a novel actuation system that is both flexible and forceful.

ACKNOWLEDGMENTS

The authors thank: Olympic Coast Seafoods LLC (Port Angeles, WA) and Cape Ann Seafood Exchange (Gloucester, MA) collected specimens of *E. stoutii* and *M. glutinosa*; Donna Downs (WA Department of Fish and Wildlife), Stacy Farina (Howard University), and Caleb Gilbert (NOAA Fisheries) facilitated and shipped specimens to Valdosta State University; Dr. Shinjiro Sueda helped align section contours with a custom MATLAB script; Austin Haney helped with animal care; and Dr. Theresa Grove provided valuable comments (as an MS thesis committee member for B.L.C.). This work was supported by the National Science Foundation [IOS-1354788 to T.A.U. and A.J.C.] and Valdosta State University [2017 and 2018 Graduate School Travel Grants to B.L.C.].

AUTHOR CONTRIBUTIONS

B.L.C.: Conceptual development, data collection, data analysis, data interpretation, manuscript preparation. A.J.C.: Data interpretation, funding, specimen acquisition, editing. T.A.U.: Conceptual development, data interpretation, funding, specimen acquisition, manuscript preparation, editing.

ORCID

Theodore Akira Uyeno https://orcid.org/0000-0001-8998-5595

REFERENCES

Auster, P. J., & Barber, K. (2006). Atlantic hagfish exploit prey captured by other taxa. *Journal of Fish Biology*, *68*, 618–621.

Cesarovic, N., Jirkof, P., Rettich, A., & Arras, M. (2011). Implantation of Radiotelemetry transmitters yielding data on ECG, heart rate, core body temperature, and activity in free-moving laboratory mice. *Journal of Visualized Experiments*, *57*, 3260.

Clark, A. J., Maravilla, E. J., & Summers, A. P. (2010). A soft origin for a forceful bite: Motor patterns of the feeding musculature in Atlantic hagfish, *Myxine glutinosa*. *Zoology*, *113*, 259–268.

Clark, A. J., & Summers, A. P. (2007). Morphology and kinematics of feeding in hagfish: Possible functional advantages of jaws. *Journal of Experimental Biology*, *210*, 3897–3909.

Clark, A. J., & Summers, A. P. (2012). Ontogenetic scaling of the morphology and biomechanics of the feeding apparatus in the Pacific hagfish *Eptatretus stoutii*. *Journal of Fish Biology*, *80*, 86–99.

Cole, F. J. (1907). A monograph on the general morphology of the myxinoid fishes, based on a study of *Myxine*. Part 2. The anatomy of the muscles. *Transactions of the Royal Society of Edinburgh*, *45*, 683–757.

Cole, F. J. (1913). A monograph on the general morphology of the myxinoid fishes, based on a study of *Myxine*. The anatomy of the gut and its appendages. *Transactions of the Royal Society of Edinburgh*, *49*, 293–344.

Dawson, J. A. (1963). The oral cavity, the 'jaws' and the horny teeth of *Myxine glutinosa*. In A. B. Fange & R. Fänge (Eds.), *The biology of Myxine* (pp. 231–255). Oslo: Universitetsforlaget.

Fernholm, B., Norén, M., Kullander, S. O., Quattrini, A. M., Zintzen, V., Roberts, C. D., … Kuo, C. H. (2013). Hagfish phylogeny and taxonomy, with description of the new genus *Rubicundus* (Craniata, Myxinidae). *Journal of Zooligal Systems and Evolutionary Research*, *51*, 296–307.

Fürbringer, P. (1875). Untersuchungen zur vergleichenden Anatomie der Muskulatur des Kopfskeletts der Cyclostomen. *Jenaische Zeitschrift für Naturwissenschaft*, *9*, 1–93.

Gans, C. (1974). *Biomechanics: An approach to vertebrate biology*. Ann Arbor, MI: The University of Michigan Press.

Gignac, P. M., & Kley, N. J. (2014). Iodine-enhanced micro-CT imaging: Methodological refinements for the study of the soft-tissue anatomy of post-embryonic vertebrates. *Journal of Experimental Zoology Part B Molecular and Developmental Evolution*, *322*, 166–176.

Glover, C. N., & Bucking, C. (2015). Feeding, digestion and nutrient absorption in hagfish. In S. L. Edwards & G. G. Goss (Eds.), *Hagfish biology* (pp. 299–320). Boca Raton: CRC Press.

Glover, C. N., Bucking, C., & Wood, C. M. (2011). Adaptations to in situ feeding: Novel nutrient acquisition pathways in an ancient vertebrate. *Proceedings of the Royal Society B: Biological Sciences*, *278*, 3096–3101.

Gustafson, G. (1935). On the biology of *Myxine glutinosa*. *Arkiv för Zoologi*, *28*, 1–8.

Iida, F., & Laschi, C. (2011). Soft robotics: Challenges and perspectives. *Procedia Computer Science*, *7*, 99–102.

Johnson, EW. (1994). Aspects of the biology of Pacific (*Eptatretus stouti*) and Black (*Eptatretus deani*) hagfishes from Monterey Bay, California. Masters Thesis, School of Natural Sciences, California State University, Fresno, CA.

Kier, W. M. (1992). Hydrostatic skeletons and muscular hydrostats. In A. A. Biewener (Ed.), *Biomechanics (structures and systems): A practical approach* (pp. 205–231). New York, NY: IRL Press at Oxford University Press.

Kier, W. M., & Smith, K. K. (1985). Tongues, tentacles, and trunks: The biomechanics of movement in muscular-hydrostats. *Zoological Journal of the Linnean Society*, *83*, 307–324.

Leigh, K. L., Sparks, J. P., & Bemis, W. E. (2016). Food preferences of Atlantic hagfish, *Myxine glutinosa*, assessed by experimental baiting of traps. *Copeia*, *104*, 623–627.

Luther, A. (1938). Muskeln des Kopfes. Die Visceralmusculatur der Acranier, Cyclostomen und Fische. In L. Bolk, E. Göppert, E. Kallius, & W. Lubosch (Eds.), *Handbuch der vergleichenden Anatomie der Wirbeltiere* (pp. 468–479). Berlin: Urban & Schwarzenberg.

Martini, F. H. (1998). The ecology of hagfishes. In J. M. Jørgensen, J. P. Lomholt, R. E. Weber, & H. Malte (Eds.), *The biology of hagfishes* (pp. 57–77). London: Chapman and Hall.

Orsbon, C. P., Gidmark, N. J., & Ross, C. F. (2018). Dynamic musculoskeletal functional morphology: Integrating diceCT and XROMM. *Anatomical Record (Hoboken)*, *301*, 378–406.

Pace, D. S., Mussi, B., Miragliuolo, A., Vivaldi, C., & Ardizzone, G. (2016). First record of a hagfish anchored to a living bottlenose dolphin in the Mediterranean Sea. *Journal of Mammalogy*, *97*, 960–965.

Powell, P. L., Roy, R. R., Kanim, P., Bello, M. A., & Edgerton, V. R. (1984). Predictability of skeletal muscle tension from architectural determinations in Guinea pig hindlimbs. *Journal of Applied Physiology*, *57*, 1715–1721.

Rus, D., & Tolley, M. T. (2015). Design, fabrication and control of soft robotics. *Nature*, *521*, 467–475.

Shelton, R. G. J. (1978). On the feeding of the hagfish *Myxine glutinosa* in the North Sea. *Journal of the Marine Biological Association of the United Kingdom*, *58*, 81–86.

Smith, C. R., & Baco, A. R. (2003). Ecology of whale falls at the deep-sea floor. *Oceanography and Marine Biology*, *41*, 311–354.

Strahan, R. (1963). The behaviour of myxinoids. *Acta Zoologica*, *44*, 73–102.

Uyeno, T. A., & Clark, A. J. (2015). Muscle articulations: Flexible jaw joints made of soft tissues. *Integrative and Comparative Biology*, *55*, 193–204.

Uyeno, T. A., & Kier, W. M. (2005). Functional morphology of the cephalopod buccal mass: A novel joint type. *Journal of Morphology*, *264*, 211–222.

Uyeno, T. A., & Kier, W. M. (2007). Electromyography of the buccal musculature of octopus (*Octopus bimaculoides*): A test of the function of the muscle articulation in support and movement. *Journal of Experimental Biology*, *201*, 118–128.

Worthington, J. (1905). Contribution of our knowledge of the myxinoids. *The American Naturalist*, *39*, 625–663.

Zhu, S., So, J., Mays, R., Desai, S., Barnes, W. R., Pourdeyhimi, B., & Dickey, M. D. (2012). Ultrastretchable fibers with metallic conductivity using a liquid metal alloy Core. *Advanced Functional Materials*, *23*, 2308–2314.

Zintzen, V., Roberts, C. D., Anderson, M. J., Stewart, A. L., Struthers, C. D., & Harvey, E. S. (2011). Hagfish predatory behaviour and slime defense mechanism. *Scientific Reports*, *1*, 131.

How to cite this article: Clubb BL, Clark AJ, Uyeno TA. Powering the hagfish "bite": The functional morphology of the retractor complex of two hagfish feeding apparatuses. *Journal of Morphology*. 2019;280:827–840. https://doi.org/10.1002/jmor.20986